

1 **CO₂-plant effects do not account for the gap between**
2 **dryness indices and projected dryness impacts in**
3 **CMIP5 or CMIP6**

4 **Jacob Scheff¹, Justin S. Mankin^{2,4}, Sloan Coats³, and Haibo Liu⁴**

5 ¹Dept. of Geography and Earth Sciences, University of North Carolina Charlotte

6 ²Dept. of Geography and Dept. of Earth Sciences, Dartmouth College

7 ³Dept. of Earth Sciences, University of Hawaii

8 ⁴Lamont-Doherty Earth Observatory of Columbia University

9 **Key Points:**

- 10 • Climate models project much more widespread drying using the Aridity Index,
11 PDSI, or SPEI than using runoff or deep soil moisture
- 12 • This gap persists even in simulations that turn off CO₂ effects on plant physiol-
13 ogy, which were thought to be its main cause
- 14 • Thus, it must have a more basic cause than CO₂ effects on plants

15 **Abstract**

16 Recent studies have found that terrestrial dryness indices like the Palmer Drought Severity Index, Standardized Precipitation Evapotranspiration Index, and Aridity Index calculated from climate model projections are mostly negative, implying a drier land surface with future warming. Yet, the same models' prognostic runoff and bulk soil moisture projections instead feature regional signals of varying sign, suggesting that the dryness indices could overstate climate change's direct impacts. Observed trends also show this "index-impact gap."

23 Most studies have attributed this gap to the indices' omission of CO₂-driven stomatal closure. However, here we show that the index-impact gap is still wide even in model experiments that switch off CO₂ effects on plants. In these simulations, mean PDSI, Aridity Index, and SPEI still decline broadly with warming, while mean runoff and bulk soil moisture still respond more equivocally. This implies that CO₂-plant effects are not the dominant or sole reason for the index-impact gap.

29 **Plain Language Summary**

30 Climate scientists have traditionally measured "drought" and "aridity" using simple formulas based on precipitation and temperature. When these formulas are applied to computer model projections of global warming, they forecast widespread increases in dryness, due to rising temperatures. Yet, these same models also directly simulate river flow and soil moisture – and do not forecast similarly widespread declines in either. Thus, it is unclear whether the drought and aridity formulas are relevant under climate change.

36 Most existing studies that examine this discrepancy blame the effect of increasing CO₂ on the microscopic pores, called stomata, that help plants conserve water. However, other studies point to more fundamental differences between the drought formulas and the direct simulations. In the present study, we show that the discrepancy persists even in special global warming simulations in which CO₂ effects on stomata are eliminated. This suggests that CO₂ effects on plants are far from the only cause of the discrepancy, and that more work needs to be done to understand it.

43 **1 Introduction**

44 *Drought* is a surface water shortage, usually driven by below-normal precipitation (P), that negatively impacts water resource production (i.e., stream runoff and groundwater recharge) and/or photosynthesis, with societal consequences (e.g., Wilhite & Glantz, 1985; AMS Council, 2013). *Aridity* is a permanent, climatological lack of enough P to support plentiful regional water resources or vegetation (Budyko & Miller, 1974; Middleton & Thomas, 1997), which plays a key role in human settlement patterns (e.g., Seager et al., 2018).

51 However, because water resource production and photosynthesis are strongly constrained by the evaporative environment as well as P , the most effective methods for quantifying aridity and drought from climate data require both P and potential evaporation E_0 . E_0 integrates radiation, temperature, humidity, and wind speed to quantify the rate at which the atmosphere is capable of evaporating surface water (e.g., Hartmann, 2016). The aridity index or AI (Transeau, 1905; Middleton & Thomas, 1997) is the ratio P/E_0 of annual climatological means. The Standardized Precipitation-Evapotranspiration Index or SPEI (Vicente-Serrano et al., 2010) is the difference $P - E_0$ smoothed to a user-defined timescale and transformed to a normal distribution. The Palmer Drought Severity Index or PDSI (Palmer, 1965) is a bucket model of soil moisture forced by monthly P and E_0 . Lower AI and more negative PDSI and SPEI values indicate drier conditions,

62 with reduced water resources and vegetation. These indices are widely used and under-
63 stood.

64 According to the standard Penman-Monteith equation (Monteith, 1981; R. G. Allen
65 et al., 1998), E_0 substantially increases with greenhouse warming, mainly due to its de-
66 pendence on temperature (Scheff & Frierson, 2014). Since projected changes in land P
67 with warming are much less robust (e.g., IPCC, 2013; Greve & Seneviratne, 2015), global-
68 scale climate model studies of AI (Feng & Fu, 2013; Fu & Feng, 2014; Scheff & Frierson,
69 2015; Huang et al., 2015; Fu et al., 2016; Zarch et al., 2017; Park et al., 2018; Wang et
70 al., 2020), PDSI (Dai, 2013; B. I. Cook et al., 2014; Zhao & Dai, 2015, 2016; Lehner et
71 al., 2017), and SPEI (B. I. Cook et al., 2014; Touma et al., 2015; Naumann et al., 2018)
72 almost always obtain widespread drying in warming scenarios. The same models also project
73 widespread declines in near-surface soil moisture SM_s (Dai, 2013; IPCC, 2013; Berg et
74 al., 2017) and relative humidity RH (IPCC, 2013; Byrne & O’Gorman, 2016), which are
75 used to argue for the physical relevance of the AI- or PDSI-based drying (e.g., Sherwood
76 & Fu, 2014; Dai et al., 2018).

77 Yet, as argued above, the core purpose of AI, PDSI, and SPEI, and the main use
78 of SM_s , is to indicate negative impacts to water-resource production and/or photosyn-
79 thesis (Roderick et al., 2015; Greve et al., 2017; Scheff et al., 2017; Scheff, 2018). And,
80 the same models that project widespread global declines in AI, PDSI, SPEI, SM_s , and
81 RH with warming project much more equivocal, two-sided changes in water-resource gen-
82 eration (IPCC, 2013; Roderick et al., 2015; Zhao & Dai, 2015, 2016; Swann et al., 2016;
83 Milly & Dunne, 2016, 2017; Greve et al., 2017; Scheff et al., 2017) and deep-layer soil
84 moisture SM_d (Berg et al., 2017; Berg & Sheffield, 2018; Greve et al., 2019). Further-
85 more, these models project ubiquitous *increases* in photosynthesis (Greve et al., 2017,
86 2019; Scheff et al., 2017; Mankin et al., 2018) and leaf coverage (Mankin et al., 2019),
87 a.k.a. “greening.” Thus, it is not clear if the AI, PDSI, and SPEI projections are actu-
88 ally relevant for warming impacts on water availability, nor (likewise) if the models’ pro-
89 gnostic runoff, SM_d , and/or vegetation projections are reliable. Scheff (2018) and Scheff
90 et al. (2017) show that this “index-impact gap” is also clear in global *observations* dur-
91 ing CO₂-driven climate changes (both recent and geologic), lending it additional credence.
92 However, it is much less pronounced in certain regions, such as the American Southwest
93 (B. I. Cook et al., 2015; Ault et al., 2016), particularly for SM_d .

94 What is the reason for this discrepancy? Most of the above studies argue that AI,
95 PDSI and SPEI do not resemble projected climate change impacts in many places mainly
96 because they do not account for the beneficial effect of elevated CO₂ on plant water re-
97 quirements, which tends to reduce evapotranspiration (ET) and increase photosynthe-
98 sis (Roderick et al., 2015; Swann et al., 2016; Greve et al., 2017, 2019; Milly & Dunne,
99 2017; Scheff et al., 2017). Yang et al. (2019, 2020) modify the standard Penman-Monteith
100 equation to include this stomatal effect and find that the resulting AI and PDSI come
101 much closer to the models’ hydrologic projections, and Lemordant et al. (2018) show that
102 CO₂-plant effects dramatically alter key model hydrologic outputs. Certainly, the bulk
103 of simulated greening would not occur without these simulated CO₂ effects (Arora et al.,
104 2013; Shao et al., 2013).

105 However, many other proposed causes of the index-impact gap, especially with re-
106 gard to hydrologic impacts (i.e., water resources and SM_d), are unrelated to CO₂-plant
107 effects. Zhao and Dai (2015), Dai et al. (2018), and Mankin et al. (2018) argue that the
108 gap occurs partly because the increase in instantaneous P rate in a warming world drives
109 greater runoff production for the same long-term total P . Observed and projected shifts
110 in P towards the hydrological wet season (e.g., Chou et al., 2013; R. J. Allen & Ander-
111 son, 2018) would have the same effect, and Berg et al. (2017) argue that the gap between
112 SM_d and SM_s also stems from rectification of the seasonal cycle. Massmann et al. (2019)
113 show that warming itself may reduce ET by closing stomata (Novick et al., 2016), apart
114 from CO₂. Further, Mankin et al. (2019) find that in much of the mid-latitudes, the pro-

115 jected increase in leaf area due to CO₂ and warming cancels any plant water savings from
 116 CO₂-induced stomatal closure, so that the net hydrologic impact of CO₂-plant effects
 117 is often negative, not positive. Lehner et al. (2019) argue that prognostic runoff responses
 118 to climate change are biased positive, because model runoff seems to be too sensitive to
 119 P , and not sensitive enough to warming. Finally, Milly and Dunne (2016) and Vicente-
 120 Serrano et al. (2019) argue that Penman-Monteith E_0 (and thus AI, PDSI and SPEI)
 121 is not always relevant to real watersheds under climate change, regardless of CO₂ effects.

122 Thus, it is not at all clear that CO₂-plant effects are the main reason why simu-
 123 lated and observed mean hydrologic impacts of climate change are not as negative as AI,
 124 PDSI, or SPEI in many regions. Indeed, Milly and Dunne (2016) found that in one model,
 125 the gap between AI and runoff responses persisted even when those effects were switched
 126 off, at least in the global average. Here, we extend that comparison to many more mod-
 127 els, variables, and regions, showing that even when CO₂-plant effects are suppressed, mean
 128 AI, PDSI, and SPEI (index) projections are much more widely negative than mean runoff,
 129 SM_d, or vegetation (impact) projections.

130 2 Data and methods

131 We examine monthly output equatorward of 55° from 11 climate models in the Cou-
 132 pled Model Intercomparison Project phase 6 (CMIP6; Eyring et al., 2016), listed in Ta-
 133 ble S1 in the Supporting Information. We compare the results of two experiments that
 134 strongly warm the planet by increasing CO₂ 1% per year for 140 years (or more). In ex-
 135 periment “1pctCO2”, both the vegetation and radiation schemes “see” the increasing
 136 CO₂, as in the experiments discussed in Section 1. Experiment “1pctCO2-rad” (Jones
 137 et al., 2016) is identical to 1pctCO2 except that the vegetation schemes instead “see”
 138 a constant 280 ppm of CO₂, so any index-impact gap in 1pctCO2-rad must occur for a
 139 reason *other* than simulated CO₂-plant effects.

140 For each model, the climatological annual-mean responses of P , E_0 , AI, PDSI, SPEI,
 141 RH, SM_s, SM_d, water resource generation (i.e., total runoff Q), runoff ratio Q/P , pho-
 142 tosynthesis, leaf area index LAI, and evaporative fraction EF are quantified using the
 143 difference between years 111-140 and years 1-30 of the “r1i1p1” run, except where noted
 144 in Table S1. Monthly E_0 is computed using the standard Penman-Monteith equation (R. G. Allen
 145 et al., 1998) and AI for each 30-year period is the ratio of 30-year-mean P to 30-year-
 146 mean E_0 , all as in Scheff et al. (2017). PDSI and 12-month SPEI are computed from monthly
 147 P and E_0 as in B. I. Cook et al. (2014) using years 1-30 as the reference period; SPEI
 148 is set to -2.33 (100-year drought) when $P-E_0$ is less than the origin of the reference
 149 distribution (S. Vicente-Serrano, pers. comm.). As in Scheff et al. (2017), monthly RH
 150 is defined as monthly-mean vapor pressure divided by saturation vapor pressure at monthly-
 151 mean temperature, for consistency with the E_0 calculation.

152 SM_s uses the “mrsos” output (mm of water in the top 10 cm of the soil), and SM_d
 153 is derived by summing the “mrlsl” output (mm of water in each soil layer) to a depth
 154 of 2 m, using a fraction of the bottom layer if necessary. They are each converted to vol-
 155 umetric water content (m³/m³), by dividing by 100 mm and 2000 mm respectively. Q
 156 is calculated as P minus ET rather than using model runoff output, to emphasize to-
 157 tal water-resource generation and avoid inconsistencies in how models defined runoff. Q/P ,
 158 which AI predicts in the present climate (Gentine et al., 2012), is the ratio of 30-year
 159 means. Photosynthesis is quantified using gross primary productivity (GPP), which is
 160 the flux of carbon through the stomata (Bonan, 2015) and thus the most water-linked
 161 metric. EF, a close cousin of the Bowen ratio, is the fraction of the 30-year-mean total
 162 turbulent heat flux (LH+SH) made up by the latent heat flux LH; decreases in EF rep-
 163 resent drought impacts to the atmosphere.

164 For each variable, the responses are nearest-neighbor interpolated to a common 3°
 165 grid, and multi-model statistics are taken. For SM_d , only nine models are available (Ta-
 166 ble S1); restricting the remainder of the study to only those models does not substan-
 167 tially change the results below. We also conduct a similar analysis on the CMIP5 (Taylor
 168 et al., 2012) 1pctCO₂ vs. “esmFdbk1” experiments, with details and results in the Sup-
 169 porting Information.

170 3 Results

171 Fig. 1 maps the median responses to the “standard” 1pctCO₂ experiment, in which
 172 both climate and vegetation respond to the CO₂ increase. The index-impact gap com-
 173 mon to the coupled models is apparent: RH, AI, SPEI, PDSI, and SM_s (Figs. 1a-e) ro-
 174 bustly and widely decline, but EF, SM_d , Q/P , and Q respond much more heterogeneously
 175 (i.e., more like P ; Figs. 1f-j), and LAI and GPP robustly and near-ubiquitously increase
 176 (Figs. 1k-l.) However, EF still resembles PDSI in some places, facially suggesting that
 177 PDSI could be relevant for atmospheric impacts (Dai et al., 2018) despite its dissimilarity
 178 to water-resource and ecological impacts. Fig. S1 in the Supporting Information re-
 179 produces Fig. 1 but using standardized changes; results are similar, except that Q and
 180 Q/P responses become much weaker than the other metrics, reinforcing the sense of a
 181 gap.

182 Fig. 2 maps the responses to the 1pctCO₂-rad experiment, in which climate responds
 183 to the CO₂ increase, but vegetation does not. Despite the lack of any CO₂-plant effects,
 184 the index-impact gap is still wide, especially for hydrologic impacts: RH, AI, SPEI, PDSI,
 185 and SM_s (Figs. 2a-e) again show widespread robust declines, but the responses of Q/P
 186 (Fig. 2h) and especially Q (Fig. 2j) are again much more two-sided. In particular, the
 187 Americas are dominated by AI, SPEI, and PDSI “drying”, yet have less consistent de-
 188 creases in Q/P , and regional decreases and increases in Q . In Africa and Australia, Q
 189 and Q/P increases are actually more extensive than decreases, despite strongly drying
 190 AI, PDSI and SPEI. However, in general, the gap is not quite as large as in Fig. 1, both
 191 because RH, AI, SPEI, and PDSI dry slightly less, and because Q and Q/P dry slightly
 192 more, consistent with Swann et al. (2016). Thus, CO₂ effects still appear to cause some
 193 of the gap, by reducing ET and thus increasing both E_0 and Q in Fig. 1 relative to Fig.
 194 2 (Berg et al., 2016; Brutsaert & Parlange, 1998).

195 SM_d (Fig. 2g) declines more robustly than Q , but not always as robustly as AI or
 196 SPEI, especially in Eurasia, North America and Australia. The declines are still weaker
 197 and less consistent than those in SM_s (Fig. 2e). Interestingly, EF (Fig. 2f) responds much
 198 more like P (Fig. 2i) than like the indices, SM_s , or even SM_d , implying that the relative
 199 consistency of EF with PDSI in Fig. 1 may just be a fortuitous effect of CO₂ reducing
 200 ET. Finally, as expected, LAI and GPP (Figs. 2k-l) lose their large, near-ubiquitous in-
 201 creases, but still change little (or even increase) in many regions where AI, SPEI and PDSI
 202 strongly decline, particularly in the mid-latitudes and Australia. Fig. S2 reproduces Fig.
 203 2 using standardized changes; again the main difference is relative weakening of the Q
 204 and Q/P responses.

205 Fig. 3 distills Figs. 1 and 2 by plotting each panel as a single point in area-with-
 206 robust-drying vs. area-with-robust-wetting space, color-coded by type of metric (where
 207 “robust” means stippled on Fig. 1 or 2; that is, $\geq 75\%$ intermodel agreement). It is im-
 208 mediately apparent that while the gap between the index (AI, PDSI, SPEI) and hydro-
 209 logic impact (Q , Q/P) projections is larger with CO₂-plant effects on (left), it is still large
 210 even with CO₂-plant effects turned off (right). In the latter case, for PDSI, more than
 211 four times as much land area has robust drying as robust wetting, yet the areas of ro-
 212 bust Q increase and robust Q decrease are equal (Fig. 3, right), complicating the inter-
 213 pretation of PDSI as a water-resource proxy under climate change (e.g., E. R. Cook et
 214 al., 2009). For AI, more than 10 times as much land area has robust drying as robust

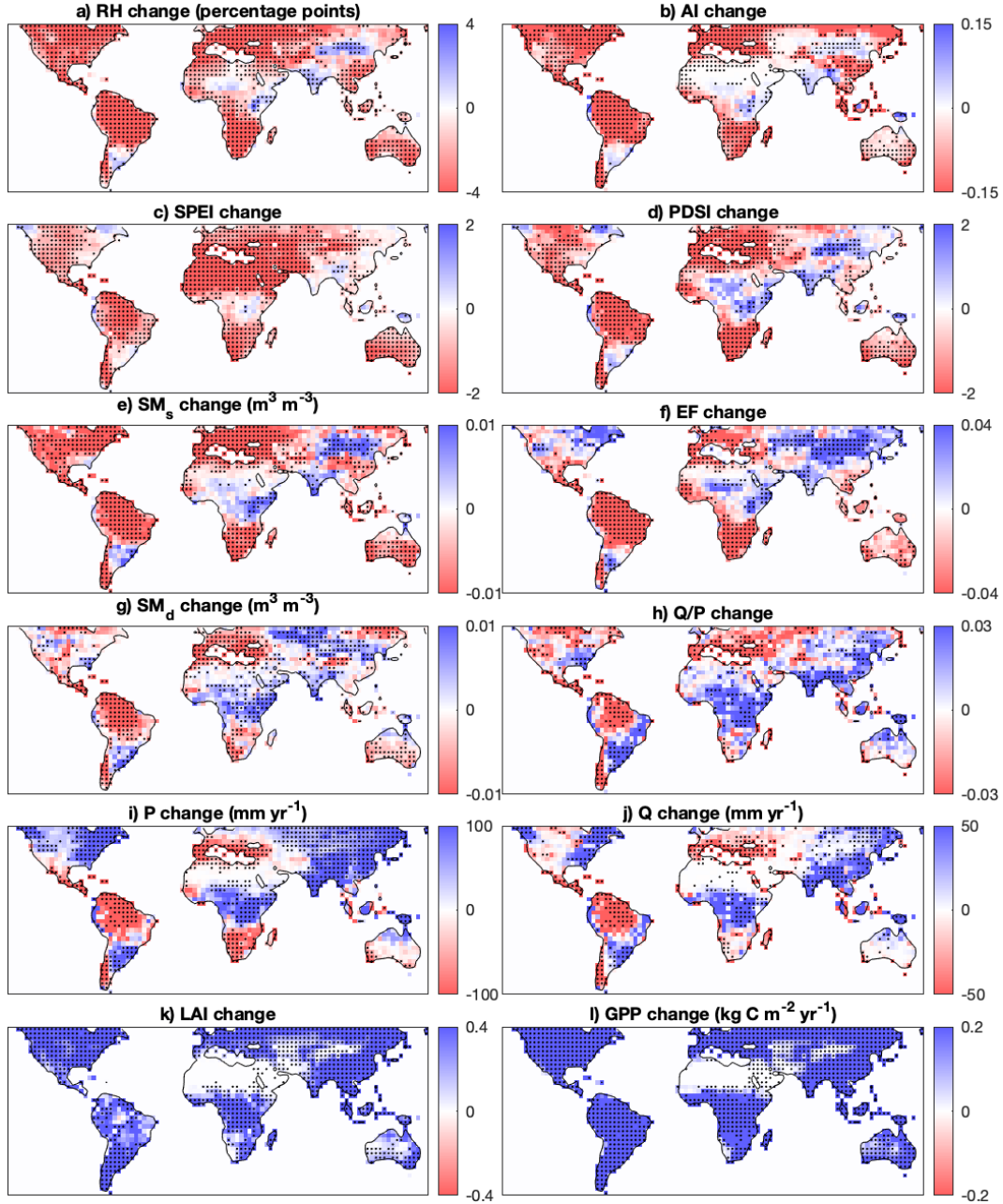


Figure 1. Multi-model median differences between years 111-140 vs. 1-30 of the 1pctCO₂ CMIP6 experiment, in which vegetation responds to the CO₂ increase. Black dots show where at least 75% of the models agree on the sign of the change (i.e., where the change is robust.) Variables without units are dimensionless.

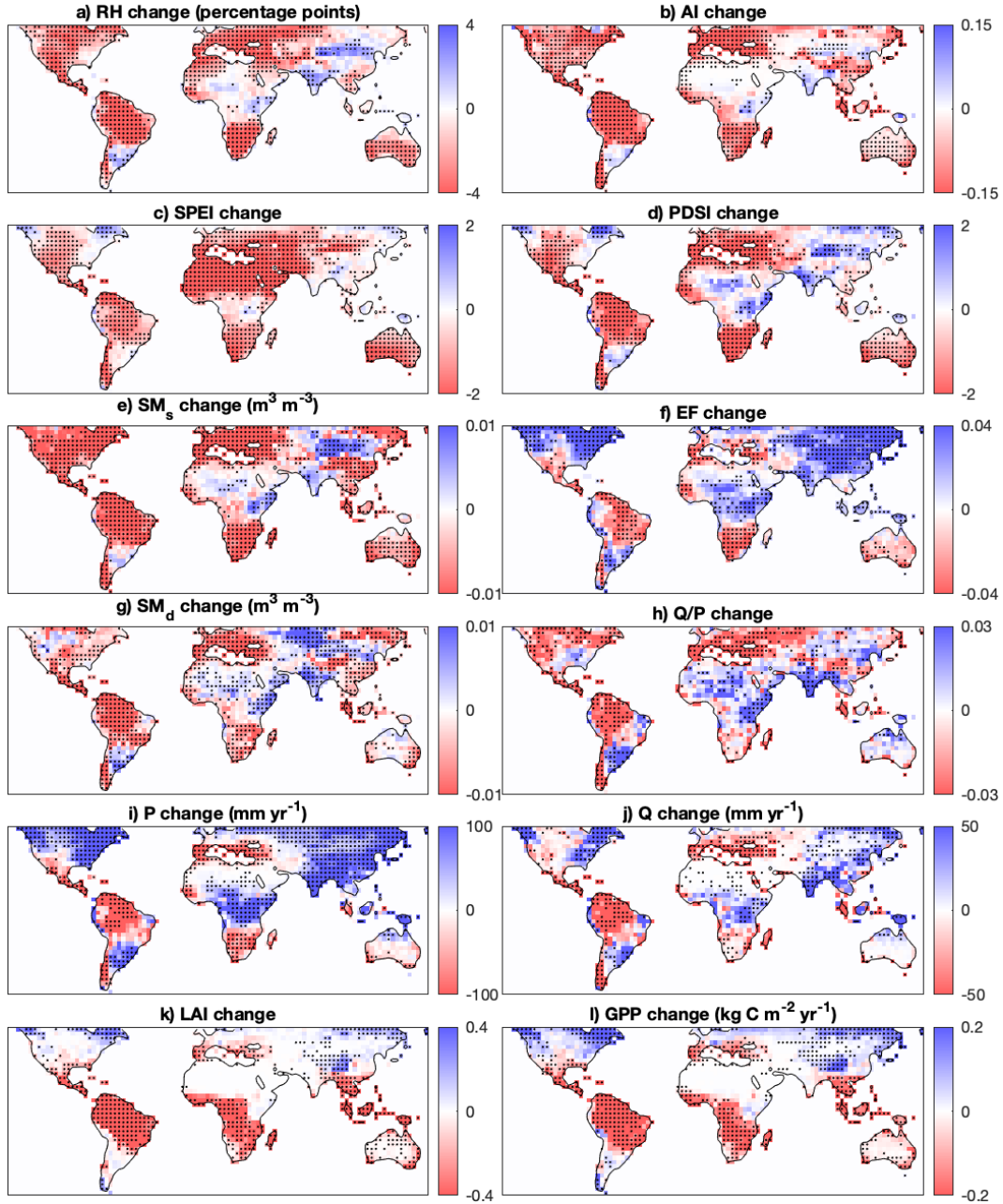


Figure 2. As Fig. 1, but for the 1pctCO₂-rad experiment, in which vegetation does not “see” the CO₂ increase.

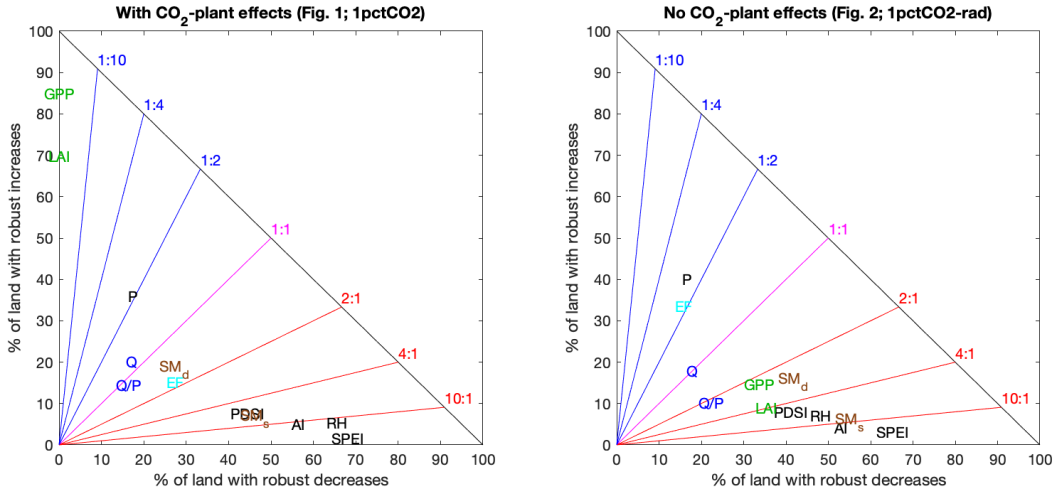


Figure 3. Percent of land area with multi-model robustly projected (i.e., stippled) decreases (x-axis) and increases (y-axis) in each variable on Fig. 1 (left; vegetation responds to CO₂) and Fig. 2 (right; vegetation does not respond to CO₂). Climate variables and indices are in black, vegetation impacts in green, water-resource impacts in dark blue, soil moisture impacts in brown, and atmospheric impacts in light blue. Colored lines mark ratios of robust-decrease area to robust-increase area.

wetting, yet the area of robust Q/P decrease is only twice the area of robust Q/P increase, despite the theoretical basis for AI as the primary driver of Q/P variation in the present climate (Budyko & Miller, 1974).

For SM_d and (especially) GPP and LAI, the gap from AI, PDSI, and SPEI responses without CO₂-plant effects (right) is much smaller than with CO₂-plant effects (left), mainly because the massive GPP and LAI increases are much reduced. However, the gap is still noticeable: similar to Q/P , robust GPP and SM_d decreases are only about 2-3 times more widespread than respective increases, even though robust PDSI, AI and SPEI decreases are over 4, 10, and 20 times more widespread than respective increases. LAI more strongly tends to decrease, similar to PDSI, but still not as much as AI, SM_s or SPEI. Thus, the indices still do not seem to be particularly reliable proxies for projected vegetation-related impacts, even in a world where CO₂ does not affect vegetation. As discussed above in the context of Fig. 1, this is particularly so in parts of the midlatitudes, where growing-season lengthening is an important driver of vegetation increases (e.g., Mankin et al., 2018, 2019). Also, EF is even farther from the indices when CO₂-plant effects are off (right) than on (left), confirming that any apparent relevance of the indices for EF in Fig. 1 is just a fortuitous consequence of CO₂ effects on transpiration.

We quantify several of the index-impact gaps in greater detail by mapping disagreement between the impact variables (Q , Q/P , SM_d, GPP) and the indices and similar variables (AI, PDSI, SPEI, SM_s) across the multi-model ensemble (Fig. 4). Specifically, we map the percentage of models that obtain increases in impact variables despite decreases in index-type variables (minus the percentage that do the opposite, which is much smaller). With CO₂-plant effects on (left column), a large proportion of the models simulate hydrologic and vegetation increases despite declining indices, as expected (though there are also regional exceptions). With CO₂-plant effects turned off (right column), this proportion persists, albeit slightly diminished. Again, the gaps between Q and Q/P and the indices (Fig. 4a-f) and between SM_d and SM_s (Fig. 4g-h) are particularly persistent. (Some very dry regions do have the opposite sign gap, but $Q \approx 0$ in such places.)

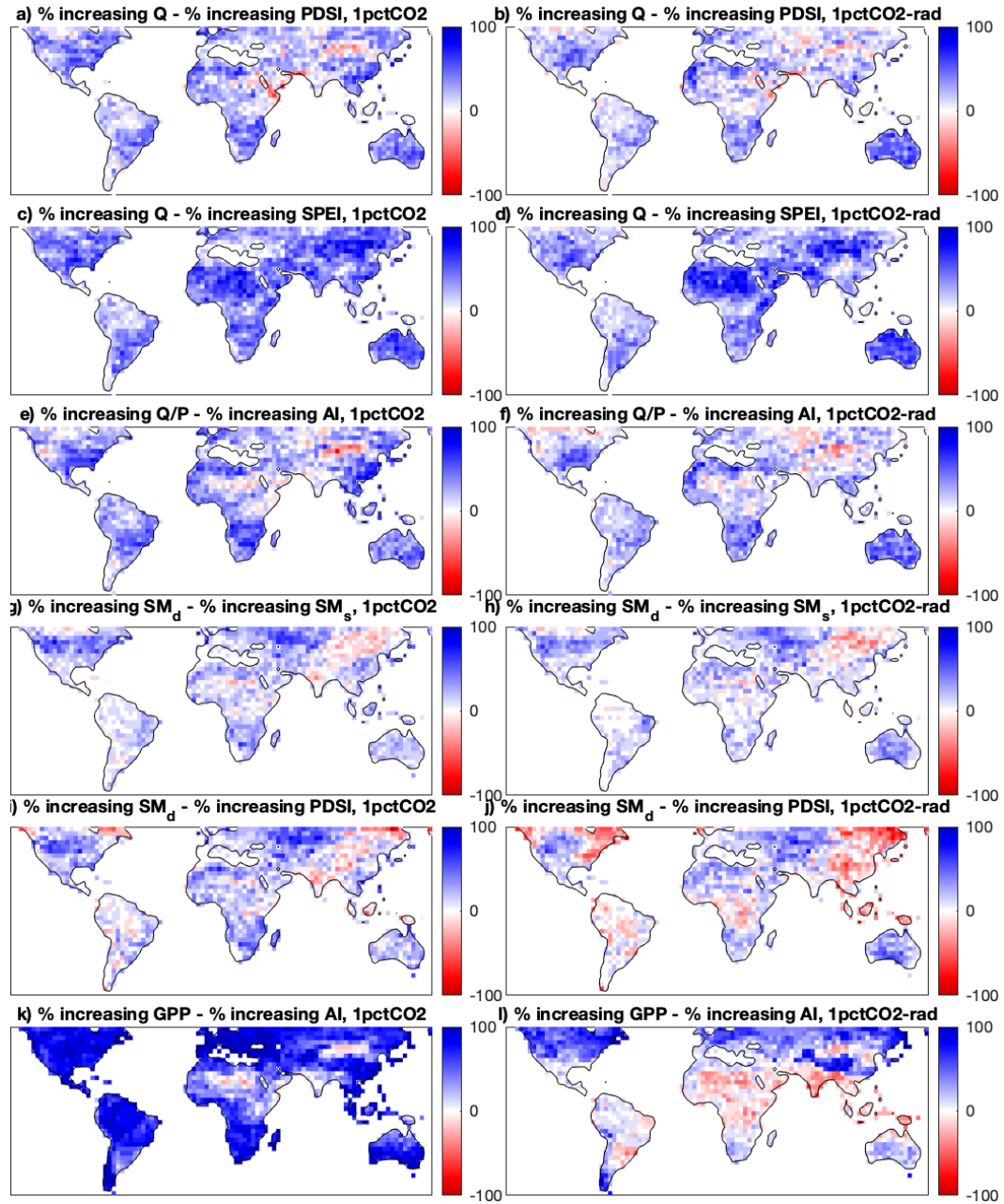


Figure 4. Percent of models with increasing A minus percent of models with increasing B (equivalently, percent of models with increasing A and declining B minus percent of models with increasing B and declining A), for selected pairs of variables A and B. Left: 1pctCO2 (vegetation sees CO₂). Right: 1pctCO2-rad (vegetation does not see CO₂). In panels g through j, both variables use only the 9 models that had SM_d for both experiments (Table S1).

In contrast, the prevalence of SM_d increases despite PDSI declines (Fig. 4i) is more noticeably reduced once CO_2 effects are turned off (Fig. 4j), while regions with the opposite sign gap are expanded. This relative agreement makes sense, since PDSI is a fundamentally a model of SM_d . Finally, the very large proportion of models that increase GPP despite index declines (e.g., Fig. 4k) largely vanishes or reverses in the tropics when CO_2 effects are turned off, but still noticeably persists in the mid-latitudes (Fig. 4l); results are similar for LAI. This again suggests that growing-season lengthening, in addition to CO_2 , is a key driver of the gap between index and vegetation responses in the midlatitudes.

Figs. S3-S6 reproduce Figs. 1-4 but using nine CMIP5 models, for cleaner comparison with the literature cited in the Introduction. The results are very similar, though the index-impact gaps (both with and without CO_2) tend to be even wider in CMIP5 than in CMIP6. Whether this is due to model improvement going from CMIP5 to CMIP6, or just different model selection (Table S1 vs. S2), is unknown. The lack of index-impact gaps in CMIP5 in parts of the American Southwest (B. I. Cook et al., 2015; Ault et al., 2016) is also apparent on Fig. S6.

4 Discussion

In short, Figs. 1-4 and S3-S6 show that while some simulated index-impact gaps can be driven by CO_2 -plant effects (e.g. low-latitude greening despite index declines, or PDSI declining more than SM_d), most of the others (e.g. Q , Q/P and mid-latitude vegetation increasing despite index declines, and SM_d declining less than SM_s) persist without any CO_2 -plant effects. Thus, contrary to studies like Swann et al. (2016), Milly and Dunne (2017), Scheff et al. (2017), and Greve et al. (2017), but in agreement with Mankin et al. (2019) and Greve et al. (2019), we find that CO_2 -plant effects are *not* the sole or dominant reason that impact simulations disagree with common climatic dryness indices under global warming. Instead, other mechanisms must be in play to explain the index-impact gaps.

What could those other, non- CO_2 factors be? The easiest explanations are that the indices are just simple formulas, and should not be expected to reflect complex climate change impacts in the first place (e.g., Milly & Dunne, 2016; Greve et al., 2019) - and/or that mean changes in runoff and vegetation production are not actually what the indices are built to measure. However, the indices all have long histories of successful use in the present climate as hydrological and ecological impact proxies, continue to be frequently used to quantify climate change's broad dryness effects (e.g., Lehner et al., 2017; Naumann et al., 2018; Wang et al., 2020), rest on solid theoretical foundations (Penman-Monteith E_0 , the Budyko curve, soil moisture modeling, the complementary principle), and do in fact agree with the impact projections in some places (Figs. 4 and S6; B. I. Cook et al., 2015; Ault et al., 2016). Where there are disagreements, they are mostly in one direction (indices drier than simulated impacts; Fig. 4) even with CO_2 effects turned off. Thus, it is important to understand where the differences come from, so as to better assess the relevance and applicability of both types of projections.

For water-resource (Q and Q/P) responses, there is no shortage of potential non- CO_2 mechanisms by which they could skew more positive than index responses, as detailed in Section 1. Again, these include direct closure of leaf stomata by high temperatures and vapor-pressure deficits (Novick et al., 2016; Massmann et al., 2019), concentration of P into fewer, heavier events (e.g., Mankin et al., 2018; Dai et al., 2018), and concentration of P into the hydrological wet season (e.g., Chou et al., 2013), all of which are accounted for in the models but not in the indices. Biases in model Q and Q/P sensitivity to P and temperature (Lehner et al., 2019) could also be important. More broadly, some of the gap between Q and PDSI responses could also simply be that PDSI is a soil-moisture model, despite its frequent tacit use to indicate runoff scarcity. However, there

294 is no similar “apples and oranges” argument for the large gap between Q/P and AI re-
 295 sponses, since Q/P is the quantity that AI classically predicts (Gentine et al., 2012; Budyko
 296 & Miller, 1974). Planned offline land-modeling work will test many of the above mech-
 297 anisms.

298 For vegetation-related impacts (GPP and LAI), the substantial non-CO₂ portion
 299 of the simulated departure from the indices is most easily explained by the lengthening
 300 of mid-latitude growing seasons with global warming (e.g., Mankin et al., 2019), as stated
 301 in Section 3. Whether a longer growing season could overcome increased drought stress
 302 to cause greening in the real-world midlatitudes absent CO₂ effects is far from certain.
 303 However, observations to date (Zhu et al., 2016) show that greening has been much more
 304 prevalent than de-greening at all latitudes, including the mid-latitudes.

305 Finally, the almost total persistence of the gap between SM_d and SM_s responses
 306 when CO₂ effects are turned off strongly suggests that its main cause is the seasonal mech-
 307 anism proposed by Berg et al. (2017), rather than plant savings of SM_d due to elevated
 308 CO₂. Similarly, the gap between EF and index responses is even stronger when CO₂ ef-
 309 fects are off, so it must have a non-CO₂ cause, likely the basic thermodynamic EF in-
 310 crease with warming and/or the strong constraint of EF by radiation and P (Scheff, 2018).

311 5 Conclusion

312 A number of studies find that simple climatic dryness and drought indices, such
 313 as the Aridity Index (AI), Palmer Drought Severity Index (PDSI), and Standardized Precipitation-
 314 Evapotranspiration Index (SPEI), indicate much more widespread drying with climate
 315 change than implied by high-complexity models (and observations) of water resources
 316 and vegetation. Many of these studies ascribe this “index-impact gap” to the direct ef-
 317 ffects of CO₂ on plant physiology. To the contrary, here we show that much of this gap
 318 strongly persists even in specialized simulations (CMIP6 1pctCO2-rad; CMIP5 esmFdbk1)
 319 in which direct CO₂-plant effects are completely *turned off*, especially for impacts on wa-
 320 ter resources and mid-latitude vegetation. This strongly suggests key non-CO₂ cause(s)
 321 for the index-impact gap. Future work will test several candidate causes from the lit-
 322 erature, using land-modeling experiments.

323 Acknowledgments

324 We acknowledge the World Climate Research Programme, which, through its Working
 325 Group on Coupled Modelling, coordinated and promoted CMIP6 and CMIP5. We thank
 326 the climate modeling groups for producing and making available their model output, the
 327 Earth System Grid Federation (ESGF) for archiving the data and providing access, and
 328 the multiple funding agencies who support CMIP and ESGF. All data is freely available
 329 at <https://esgf-node.llnl.gov/search/cmip6/> and <https://esgf-node.llnl.gov/search/cmip5/>. J. S. was supported by a UNC Charlotte Faculty Research Grant in 2019-
 330 20.

332 References

- 333 Allen, R. G., Pereira, L. S., Raes, D., & Smith, M. (1998). *Crop evapotranspiration:*
 334 *guidelines for computing crop water requirements* (Irrigation and Drainage
 335 Paper No. 56). Food and Agriculture Organization.
 336 Allen, R. J., & Anderson, R. G. (2018). 21st century California drought risk linked
 337 to model fidelity of the El Niño teleconnection. *NPJ Climate and Atmospheric
 338 Science*, 1, 21. doi: 10.1038/s41612-018-0032-x
 339 AMS Council. (2013). *Drought: an information statement of the American Meteo-*
 340 *rological Society*. Retrieved from [https://www.ametsoc.org/ams/index.cfm/](https://www.ametsoc.org/ams/index.cfm/about-ams/ams-statements/statements-of-the-ams-in-force/drought/)
 341 [about-ams/ams-statements/statements-of-the-ams-in-force/drought/](https://www.ametsoc.org/ams-statements/statements-of-the-ams-in-force/drought/)

- 342 Arora, V. K., Boer, G. J., Friedlingstein, P., Eby, M., Jones, C. D., Christian, J. R.,
 343 ... Wu, T. (2013). Carbon-concentration and carbon-climate feedbacks
 344 in CMIP5 earth system models. *Journal of Climate*, *26*, 5289-5314. doi:
 345 10.1175/JCLI-D-12-00494.1
- 346 Ault, T. R., Mankin, J. S., Cook, B. I., & Smerdon, J. E. (2016). Relative impacts
 347 of mitigation, temperature, and precipitation on 21st-century megadrought
 348 risk in the American Southwest. *Science Advances*, *2*, e1600873. doi:
 349 10.1126/sciadv.1600873
- 350 Berg, A., Findell, K., Lintner, B., Giannini, A., Seneviratne, S. I., B. van den Hurk,
 351 ... Milly, P. C. D. (2016). Land-atmosphere feedbacks amplify aridity increase
 352 over land under global warming. *Nature Climate Change*, *6*, 869-874. doi:
 353 10.1038/nclimate3029
- 354 Berg, A., & Sheffield, J. (2018). Climate change and drought: the soil moisture per-
 355 spective. *Current Climate Change Reports*, *4*, 180-191. doi: 10.1007/s40641
 356 -018-0095-0
- 357 Berg, A., Sheffield, J., & Milly, P. C. D. (2017). Divergent surface and total soil
 358 moisture projections under global warming. *Geophysical Research Letters*, *44*,
 359 236-244. doi: 10.1002/2016GL071921
- 360 Bonan, G. (2015). *Ecological climatology: concepts and applications* (3rd ed.). Cam-
 361 bridge University Press. doi: 10.1017/CBO9781107339200
- 362 Boucher, O., Denvil, S., Caubel, A., & Foujols, M. A. (2018a). *IPSL IPSL-CM6A-*
363 LR model output prepared for CMIP6 C4MIP 1pctCO2-rad. Version 20180914.
 364 Earth System Grid Federation. doi: 10.22033/ESGF/CMIP6.5051
- 365 Boucher, O., Denvil, S., Caubel, A., & Foujols, M. A. (2018b). *IPSL IPSL-CM6A-*
366 LR model output prepared for CMIP6 CMIP 1pctCO2. Version 20180727.
 367 Earth System Grid Federation. doi: 10.22033/ESGF/CMIP6.5049
- 368 Brovkin, V., Wieners, K.-H., Giorgetta, M., Jungclaus, J., Reick, C., Esch, M., ...
 369 Roeckner, E. (2019). *MPI-M MPI-ESM1.2-LR model output prepared for*
370 CMIP6 C4MIP 1pctCO2-rad. Version 20190710. Earth System Grid Federa-
 371 tion. doi: 10.22033/ESGF/CMIP6.6439
- 372 Brutsaert, W., & Parlange, M. B. (1998). Hydrologic cycle explains the evaporation
 373 paradox. *Nature*, *396*, 30.
- 374 Budyko, M. I., & Miller, D. H. (1974). *Climate and life*. Academic Press.
- 375 Byrne, M. P., & O'Gorman, P. A. (2016). Understanding decreases in land relative
 376 humidity with global warming: conceptual model and GCM simulations. *Jour-
 377 nal of Climate*, *29*, 9045-9061. doi: 10.1175/JCLI-D-16-0351.1
- 378 Chou, C., Chiang, J. C. H., Lan, C.-W., Chung, C.-H., Liao, Y.-C., & Lee, C.-J.
 379 (2013). Increase in the range between wet and dry season precipitation. *Nature*
 380 *Geoscience*, *6*, 263-267. doi: 10.1038/NGEO1744
- 381 Cook, B. I., Ault, T. R., & Smerdon, J. E. (2015). Unprecedented 21st century
 382 drought risk in the American Southwest and Central Plains. *Science Advances*,
 383 *1*, e1400082. doi: 10.1126/sciadv.1400082
- 384 Cook, B. I., Smerdon, J. E., Seager, R., & Coats, S. (2014). Global warming and
 385 21st century drying. *Climate Dynamics*, *43*, 2607-2627. doi: 10.1007/s00382
 386 -014-2075-y
- 387 Cook, E. R., Seager, R., Heim, R. R., Vose, R. S., Herweijer, C., & Woodhouse, C.
 388 (2009). Megadroughts in North America: placing IPCC projections of hydro-
 389 climatic change in a long-term palaeoclimate context. *Journal of Quaternary*
 390 *Science*, *25*, 48-61. doi: 10.1002/jqs.1303
- 391 Dai, A. (2013). Increasing drought under global warming in observations and mod-
 392 els. *Nature Climate Change*, *3*, 52-58. doi: 10.1038/NCLIMATE1633
- 393 Dai, A., Zhao, T., & Chen, J. (2018). Climate change and drought: a precipitation
 394 and evaporation perspective. *Current Climate Change Reports*, *4*, 301-312.
 395 doi: 10.1007/s40641-018-0101-6
- 396 Eyring, V., Bony, S., Meehl, G. A., Senior, C. A., Stevens, B., Stouffer, R. J., &

- Taylor, K. E. (2016). Overview of the Coupled Model Intercomparison Project Phase 6 (CMIP6) experimental design and organization. *Geoscientific Model Development*, *9*, 1937-1958. doi: 10.5194/gmd-9-1937-2016
- Feng, S., & Fu, Q. (2013). Expansion of global drylands under a warming climate. *Atmospheric Chemistry and Physics*, *13*, 10081-10094. doi: 10.5194/acp-13-10081-2013
- Fu, Q., & Feng, S. (2014). Responses of terrestrial aridity to global warming. *Journal of Geophysical Research*, *119*, 7863-7875. doi: 10.1002/2014JD021608
- Fu, Q., Lin, L., Huang, J., Feng, S., & Gettelman, A. (2016). Changes in terrestrial aridity for the period 850-2080 from the Community Earth System Model. *Journal of Geophysical Research - Atmospheres*, *121*, 2857-2873. doi: 10.1002/2015JD024075
- Gentine, P., D'Odorico, P., Lintner, B. R., Sivandran, G., & Salvucci, G. (2012). Interdependence of climate, soil, and vegetation as constrained by the Budyko curve. *Geophysical Research Letters*, *39*, L19404. doi: 10.1029/2012GL053492
- Greve, P., Roderick, M. L., & Seneviratne, S. I. (2017). Simulated changes in aridity from the last glacial maximum to 4xCO₂. *Environmental Research Letters*, *12*, 114021. doi: 10.1088/1748-9326/aa89a3
- Greve, P., Roderick, M. L., Ukkola, A. M., & Wada, Y. (2019). The aridity index under global warming. *Environmental Research Letters*, *14*, 124006. doi: 10.1088/1748-9326/ab5046
- Greve, P., & Seneviratne, S. I. (2015). Assessment of future changes in water availability and aridity. *Geophysical Research Letters*, *42*, 5493-5499. doi: 10.1002/2015GL064127
- Hartmann, D. (2016). *Global physical climatology* (2nd ed.). Elsevier.
- Huang, J., Yu, H., Guan, X., Wang, G., & Guo, R. (2015). Accelerated dryland expansion under climate change. *Nature Climate Change*, *6*, 166-171. doi: 10.1038/NCLIMATE2837
- IPCC. (2013). Long-term climate change: projections, commitments and irreversibility. In T. Stocker et al. (Eds.), *Climate change 2013: the physical science basis. Contribution of Working Group I to the Fifth Assessment Report of the Intergovernmental Panel on Climate Change* (p. 1029-1136). Cambridge University Press.
- Jones, C. D. (2019). *MOHC UKESM1.0-LL model output prepared for CMIP6 C4MIP 1pctCO2-rad. Version 20190904 for evpsbl, gpp, and lai; 20190723 for all others*. Earth System Grid Federation. doi: 10.22033/ESGF/CMIP6.5800
- Jones, C. D., Arora, V., Friedlingstein, P., Bopp, L., Brovkin, V., Dunne, J., ... Zaehle, S. (2016). C4MIP - The Coupled Climate-Carbon Cycle Model Intercomparison Project: experimental protocol for CMIP6. *Geoscientific Model Development*, *9*, 2853-2880. doi: 10.5194/gmd-9-2853-2016
- Krasting, J. P., Blanton, C., McHugh, C., Radhakrishnan, A., John, J. G., Rand, K., ... Zeng, Y. (2018). *NOAA-GFDL GFDL-ESM4 model output prepared for CMIP6 C4MIP 1pctCO2-rad. Version 20180701*. Earth System Grid Federation. doi: 10.22033/ESGF/CMIP6.8477
- Krasting, J. P., John, J. G., Blanton, C., McHugh, C., Nikonov, S., Radhakrishnan, A., ... Zhao, M. (2018). *NOAA-GFDL GFDL-ESM4 model output prepared for CMIP6 CMIP 1pctCO2. Version 20180701*. Earth System Grid Federation. doi: 10.22033/ESGF/CMIP6.8473
- Lehner, F., Coats, S., Stocker, T. F., Pendergrass, A. G., Sanderson, B. M., Raible, C. C., & Smerdon, J. E. (2017). Projected drought risk in 1.5°C and 2°C warmer climates. *Geophysical Research Letters*, *44*, 7419-7428. doi: 10.1002/2017GL074117
- Lehner, F., Wood, A. W., Vano, J. A., Lawrence, D. M., Clark, M. P., & Mankin, J. S. (2019). The potential to reduce uncertainty in regional runoff projections from climate models. *Nature Climate Change*, *9*, 926-933. doi:

- 452 10.1038/s41558-019-0639-x
- 453 Lemordant, L., Gentine, P., Swann, A. S., Cook, B. I., & Scheff, J. (2018). Critical
454 impact of vegetation physiology on the continental hydrologic cycle in response
455 to increasing CO₂. *Proceedings of the National Academy of Sciences of the
456 USA*, *115*, 4093-4098. doi: 10.1073/pnas.1720712115
- 457 Mankin, J. S., Seager, R., Smerdon, J. E., Cook, B. I., & Williams, A. P. (2019).
458 Mid-latitude freshwater availability reduced by projected vegetation re-
459 sponds to climate change. *Nature Geoscience*, *12*, 983-988. doi: 10.1038/
460 s41561-019-0480-x
- 461 Mankin, J. S., Seager, R., Smerdon, J. E., Cook, B. I., Williams, A. P., & Horton,
462 R. M. (2018). Blue water trade-offs with vegetation in a CO₂-enriched climate.
463 *Geophysical Research Letters*, *45*, 3115-3125. doi: 10.1002/2018GL077051
- 464 Massmann, A., Gentine, P., & Lin, C. (2019). When does vapor pressure deficit
465 drive or reduce evapotranspiration? *Journal of Advances in Modeling Earth
466 Systems*, *11*, 3305-3320. doi: 10.1029/2019MS001790
- 467 Middleton, N., & Thomas, D. S. G. (1997). *World atlas of desertification* (2nd ed.).
468 Wiley.
- 469 Milly, P. C. D., & Dunne, K. A. (2016). Potential evapotranspiration and continen-
470 tal drying. *Nature Climate Change*, *6*, 946-949. doi: 10.1038/nclimate3046
- 471 Milly, P. C. D., & Dunne, K. A. (2017). A hydrologic drying bias in water-resource
472 impact analyses of anthropogenic climate change. *Journal of the American
473 Water Resources Association*, *53*, 822-838. doi: 10.1111/1752-1688.12538
- 474 Monteith, J. L. (1981). Evaporation and surface temperature. *Quarterly Journal of
475 the Royal Meteorological Society*, *107*, 1-27.
- 476 NASA/GISS. (2019a). *NASA-GISS GISS-E2.1G model output prepared for CMIP6
477 C4MIP 1pctCO2-rad. Version 20190815*. Earth System Grid Federation. doi:
478 10.22033/ESGF/CMIP6.6958
- 479 NASA/GISS. (2019b). *NASA-GISS GISS-E2.1G model output prepared for CMIP6
480 CMIP 1pctCO2. Version 20190815*. Earth System Grid Federation. doi: 10
481 .22033/ESGF/CMIP6.6950
- 482 Naumann, G., Alfieri, L., Wyser, K., Mentaschi, L., Betts, R. A., Carrao, H.,
483 ... Feyen, L. (2018). Global changes in drought conditions under differ-
484 ent levels of warming. *Geophysical Research Letters*, *45*, 3285-3296. doi:
485 10.1002/2017GL076521
- 486 Novick, K. A., Ficklin, D. L., Stoy, P. C., Williams, C. A., Bohrer, G., Oishi, A. C.,
487 ... Phillips, R. P. (2016). The increasing importance of atmospheric demand
488 for ecosystem water and carbon fluxes. *Nature Climate Change*, *6*, 1023-1027.
489 doi: 10.1038/NCLIMATE3114
- 490 Palmer, W. C. (1965). *Meteorological drought* (Research Paper No. 45). U.S.
491 Weather Bureau.
- 492 Park, C.-E., Jeong, S.-J., Joshi, M., Osborn, T. J., Ho, C.-H., Piao, S., ... Feng, S.
493 (2018). Keeping global warming within 1.5 °C constrains emergence of aridifi-
494 cation. *Nature Climate Change*, *8*, 70-74. doi: 10.1038/s41558-017-0034-4
- 495 Roderick, M. L., Greve, P., & Farquhar, G. D. (2015). On the assessment of aridity
496 with changes in atmospheric CO₂. *Water Resources Research*, *51*, 5450-5463.
497 doi: 10.1002/2015WR017031
- 498 Scheff, J. (2018). Drought indices, drought impacts, CO₂, and warming: a historical
499 and geologic perspective. *Current Climate Change Reports*, *4*, 202-209. doi: 10
500 .1007/s40641-018-0094-1
- 501 Scheff, J., & Frierson, D. M. W. (2014). Scaling potential evapotranspiration with
502 greenhouse warming. *Journal of Climate*, *27*, 1539-1558. doi: 10.1175/JCLI-D
503 -13-00233.1
- 504 Scheff, J., & Frierson, D. M. W. (2015). Terrestrial aridity and its response to green-
505 house warming across CMIP5 climate models. *Journal of Climate*, *28*, 5583-
506 5600. doi: 10.1175/JCLI-D-14-00480.1

- 507 Scheff, J., Seager, R., Liu, H., & Coats, S. (2017). Are glacials dry? Consequences
 508 for paleoclimatology and for greenhouse warming. *Journal of Climate*, 30,
 509 6593-6609. doi: 10.1175/JCLI-D-16-0854.1
- 510 Swinger, J., Tjiputra, J., Seland, Ø., Bentsen, M., Olivière, D. J. L., Toniazzo, T.,
 511 ... Schulz, M. (2020). *NCC NorESM2-LM model output prepared for CMIP6*
 512 *C4MIP 1pctCO2-rad. Version 20200206.* Earth System Grid Federation. doi:
 513 10.22033/ESGF/CMIP6.13726
- 514 Seager, R., Lis, N., Feldman, J., Ting, M., Williams, A., Nakamura, J., ... Hender-
 515 son, N. (2018). Whither the 100th meridian? The once and future physical
 516 and human geography of America's arid-humid divide. Part I: The story so far.
 517 *Earth Interactions*, 22, 5. doi: 10.1175/EI-D-17-0011.1
- 518 Seferian, R. (2018a). *CNRM-CERFACS CNRM-ESM2-1 model output prepared for*
 519 *CMIP6 C4MIP 1pctCO2-rad. Version 20181113.* Earth System Grid Federa-
 520 tion. doi: 10.22033/ESGF/CMIP6.3718
- 521 Seferian, R. (2018b). *CNRM-CERFACS CNRM-ESM2-1 model output prepared*
 522 *for CMIP6 CMIP 1pctCO2. Version 20181018.* Earth System Grid Federation.
 523 doi: 10.22033/ESGF/CMIP6.3714
- 524 Seland, Ø., Bentsen, M., Olivière, D. J. L., Toniazzo, T., Gjermundsen, A., Graff,
 525 L. S., ... Schulz, M. (2019). *NCC NorESM2-LM model output prepared*
 526 *for CMIP6 CMIP 1pctCO2. Version 20191108 for sfcWind; 20190815 for*
 527 *all other Amon; 20190917 for Lmon.* Earth System Grid Federation. doi:
 528 10.22033/ESGF/CMIP6.7802
- 529 Shao, P., Xubin Zeng, Sakaguchi, K., Monson, R. K., & Xiaodong Zeng. (2013). Ter-
 530 restrial carbon cycle: climate relations in eight CMIP5 earth system models.
 531 *Journal of Climate*, 26, 8744-8764. doi: 10.1175/JCLI-D-12-00831.1
- 532 Sherwood, S., & Fu, Q. (2014). A drier future? *Science*, 343, 737-739. doi: 10.1126/
 533 science.1247620
- 534 Swann, A. L. S., Hoffman, F. M., Koven, C. D., & Randerson, J. T. (2016). Plant
 535 responses to increasing CO₂ reduce estimates of climate impacts on drought
 536 severity. *Proceedings of the National Academy of Sciences of the USA*, 113,
 537 10019-10024. doi: 10.1073/pnas.1604581113
- 538 Swart, N. C., Cole, J. N., Kharin, V. V., Lazare, M., Scinocca, J. F., Gillett, N. P.,
 539 ... Sigmond, M. (2019a). *CCCma CanESM5 model output prepared for*
 540 *CMIP6 C4MIP 1pctCO2-rad. Version 20190429.* Earth System Grid Federa-
 541 tion. doi: 10.22033/ESGF/CMIP6.3154
- 542 Swart, N. C., Cole, J. N., Kharin, V. V., Lazare, M., Scinocca, J. F., Gillett, N. P.,
 543 ... Sigmond, M. (2019b). *CCCma CanESM5 model output prepared for*
 544 *CMIP6 CMIP 1pctCO2. Version 20190429.* Earth System Grid Federation.
 545 doi: 10.22033/ESGF/CMIP6.3151
- 546 Tang, Y., Rumbold, S., Ellis, R., Kelley, D., Mulcahy, J., Sellar, A., ... Jones, C.
 547 (2019). *MOHC UKESM1.0-LL model output prepared for CMIP6 CMIP*
 548 *1pctCO2. Version 20190701 for evpsbl, gpp, and lai; 20190406 for all others.*
 549 Earth System Grid Federation. doi: 10.22033/ESGF/CMIP6.5792
- 550 Taylor, K. E., Stouffer, R. J., & Meehl, G. A. (2012). An overview of CMIP5 and
 551 the experiment design. *Bulletin of the American Meteorological Society*, 93,
 552 485-498. doi: 10.1175/BAMS-D-11-00094.1
- 553 Touma, D., Ashfaq, M., Nayak, M., Kao, S.-C., & Diffenbaugh, N. S. (2015).
 554 A multi-model and multi-index evaluation of drought characteristics in
 555 the 21st century. *Journal of Hydrology*, 526, 196-207. doi: 10.1016/
 556 j.jhydrol.2014.12.011
- 557 Transeau, E. N. (1905). Forest centers of eastern America. *Amer. Naturalist*, 39,
 558 875-889.
- 559 Vicente-Serrano, S. M., Beguería, S., & López-Moreno, J. I. (2010). A multi-
 560 scalar drought index sensitive to global warming: the standardized precip-
 561 itation evapotranspiration index. *Journal of Climate*, 23, 1696-1718. doi:

- 562 10.1175/2009JCLI2909.1
 563 Vicente-Serrano, S. M., McVicar, T. R., Miralles, D. G., Yang, Y., & Tomas-
 564 Burguera, M. (2019). Unraveling the influence of atmospheric evaporative
 565 demand on drought and its response to climate change. *WIREs Climate
 566 Change*, 11, e632. doi: 10.1002/wcc.632
- 567 Wang, X., Jiang, D., & Lang, X. (2020). Future changes in Aridity Index at two and
 568 four degrees of global warming above preindustrial levels. *International Jour-
 569 nal of Climatology*. doi: 10.1002/joc.6620
- 570 Wieners, K.-H., Giorgetta, M., Jungclaus, J., Reick, C., Esch, M., Bittner, M., ...
 571 Roeckner, E. (2019). *MPI-M MPI-ESM1.2-LR model output prepared for
 572 CMIP6 CMIP 1pctCO₂. Version 20190710*. Earth System Grid Federation.
 573 doi: 10.22033/ESGF/CMIP6.6435
- 574 Wilhite, D. A., & Glantz, M. H. (1985). Understanding the drought phe-
 575 nomenon: the role of definitions. *Water International*, 10, 111-120. doi:
 576 10.1080/02508068508686328
- 577 Wu, T., Chu, M., Dong, M., Fang, Y., Jie, W., Li, J., ... Zhang, Y. (2018). *BCC
 578 BCC-CSM2MR model output prepared for CMIP6 CMIP 1pctCO₂. Version
 579 20181012 for Lmon and 20181015 for Amon*. Earth System Grid Federation.
 580 doi: 10.22033/ESGF/CMIP6.2833
- 581 Wu, T., Chu, M., Dong, M., Fang, Y., Jie, W., Li, J., ... Zhang, Y. (2019). *BCC
 582 BCC-CSM2MR model output prepared for CMIP6 C4MIP 1pctCO₂-rad. Ver-
 583 sion 20190313 for Lmon and 20190321 for Amon*. Earth System Grid Federation.
 584 doi: 10.22033/ESGF/CMIP6.2836
- 585 Yang, Y., Roderick, M. L., Zhang, S., McVicar, T. R., & Donohue, R. J. (2019).
 586 Hydrologic implications of vegetation response to elevated CO₂ in climate pro-
 587 jections. *Nature Climate Change*, 9, 44-48. doi: 10.1038/s41558-018-0361-0
- 588 Yang, Y., Zhang, S., Roderick, M. L., McVicar, T. R., Yang, D., Liu, W., & Li, X.
 589 (2020). Comparing PDSI drought assessments using the traditional offline
 590 approach with direct climate model outputs. *Hydrology and Earth System
 591 Science*, 24, 2921-2930. doi: 10.5194/hess-24-2921-2020
- 592 Yukimoto, S., Koshiro, T., Kawai, H., Oshima, N., Yoshida, K., Urakawa, S., ...
 593 Adachi, Y. (2020a). *MRI MRI-ESM2.0 model output prepared for CMIP6
 594 C4MIP 1pctCO₂-rad. Version 20191205 for Amon and 20200313 for Lmon*.
 595 Earth System Grid Federation. doi: 10.22033/ESGF/CMIP6.5358
- 596 Yukimoto, S., Koshiro, T., Kawai, H., Oshima, N., Yoshida, K., Urakawa, S., ...
 597 Adachi, Y. (2020b). *MRI MRI-ESM2.0 model output prepared for CMIP6
 598 CMIP 1pctCO₂. Version 20191205 for Amon and 20200313 for Lmon*. Earth
 599 System Grid Federation. doi: 10.22033/ESGF/CMIP6.5356
- 600 Zarch, M. A. A., Sivakumar, B., Malekinezhad, H., & Sharma, A. (2017). Future
 601 aridity under conditions of global climate change. *Journal of Hydrology*, 554,
 602 451-469. doi: 10.1016/j.jhydrol.2017.08.043
- 603 Zhao, T., & Dai, A. (2015). The magnitude and causes of global drought changes
 604 in the twenty-first century under a low-moderate emissions scenario. *Journal of
 605 Climate*, 28, 4490-4512. doi: 10.1175/JCLI-D-14-00363.1
- 606 Zhao, T., & Dai, A. (2016). Uncertainties in historical changes and future pro-
 607 jections of drought. Part II: model-simulated historical and future drought
 608 changes. *Climatic Change*, 144, 535-548. doi: 10.1007/s10584-016-1742-x
- 609 Zhu, Z., Piao, S., Myneni, R. B., Huang, M., Zeng, Z., Canadell, J. G., ... Zeng,
 610 N. (2016). Greening of the Earth and its drivers. *Nature Climate Change*, 6,
 611 791-795. doi: 10.1038/NCLIMATE3004
- 612 Ziehn, T., Chamberlain, M., Lenton, A., Law, R., Bodman, R., Dix, M., ...
 613 Ridzwan, S. M. (2019a). *CSIRO ACCESS-ESM1.5 model output prepared
 614 for CMIP6 C4MIP 1pctCO₂-rad. Version 20191118*. Earth System Grid Feder-
 615 ation. doi: 10.22033/ESGF/CMIP6.4234
- 616 Ziehn, T., Chamberlain, M., Lenton, A., Law, R., Bodman, R., Dix, M., ... Druken,

617 K. (2019b). *CSIRO ACCESS-ESM1.5 model output prepared for CMIP6*
618 *CMIP 1pctCO₂. Version 20191115.* Earth System Grid Federation. doi:
619 10.22033/ESGF/CMIP6.4231